

Chapter 5

Understanding Irregular Satellites

Beginning with this Chapter, we start to consider various phenomena due to the LKE in astronomical and astrophysical systems. Historically, the first theoretical works on this mechanism by Lidov (1961) were devoted to planetary satellites, both natural and artificial; that is why we start with an overview of the most pronounced LK-phenomena in the satellite dynamics, namely, with the LKE in the dynamics of irregular satellites of giant planets.

For a planetary satellite, the qualitative LK-mechanism can be described as following: the secular variations in the eccentricity and inclination are coupled,¹ as integral (3.23) certifies, if the R3BP conditions are fulfilled at least approximately. The dynamical cause of the effect lies in the presence of a distant perturber; in the given case, it is the Sun, or some other massive satellite (e.g., the Moon in the Earth–Moon system). Therefore, if a satellite’s orbit is inclined initially high enough with respect to the orbital plane of the host planet, the satellite’s eccentricity may strongly (depending on initial conditions) oscillate on the secular timescale, and, when the eccentricity is maximum, the pericentric and apocentric distances are, respectively, minimum and maximum. Therefore, at the pericenter, the satellite may be destroyed by planetary tides or may collide with a large regular moon or with the planet itself. On the other hand, at the apocenter, the satellite may leave the planet’s *Hill sphere* and escape.

The Hill sphere of a planet engulfs a zone of the planet’s gravitational dominance: inside it, the planet’s gravity dominates over the Solar perturbations, and the latter cannot enforce the satellites’ escape. For example, in the Earth case, the *Hill radius* (radius of the Hill sphere) is about four (≈ 3.9) times greater than the orbital semimajor axis of the Moon, that is why the Moon is safe with us.

The Hill radius can be estimated by means of an analysis of the locations of the libration points in the three-body problem (see, e.g., Murray and Dermott 1999). In

¹They are in antiphase, if the inclination $i < \pi/2$, and in phase, if $i > \pi/2$.

a planet–Sun system, if the planet’s orbit is circular, the Hill radius is given by

$$R_{\text{H}}^{\text{circ}} = \left(\frac{m_{\text{p}}}{3m_{\text{Sun}}} \right)^{1/3} a_{\text{p}}, \quad (5.1)$$

where m_{p} and m_{Sun} are the masses of the planet and the Sun, respectively, and a_{p} is the semimajor axis of the planet’s orbit.

If the orbit of the secondary (planet) is eccentric, then the radius of the stability zone is approximately equal to $R_{\text{H}}^{\text{circ}}$ calculated at the secondary’s pericenter (Hamilton and Burns 1992):

$$R_{\text{H}} \approx \left(\frac{m_{\text{p}}}{3m_{\text{Sun}}} \right)^{1/3} a_{\text{p}}(1 - e_{\text{p}}), \quad (5.2)$$

where e_{p} is the eccentricity of the secondary. This formula expresses the so-called *Hill sphere at pericenter scaling*.

As established in astronomical observations of satellites of the giant planets (Jupiter, Saturn, Uranus, and Neptune), the satellites with orbits inside ~ 0.05 of the Hill radius of the parent planet tend to be in close-to-circular prograde equatorial orbits.² These are called “regular” satellites. Conversely, the satellites with orbits outside ~ 0.05 of the Hill radius tend to have large eccentricities and inclinations, and many are retrograde. These are called “irregular” satellites.

A more rigorous definition can be adopted: Nesvorný et al. (2003) define an *irregular* as a satellite that has the orbital semimajor axis large enough for the precession of the satellite’s orbit to be controlled by the Sun, not by the parent planet’s oblateness; i.e., the Solar perturbations dominate over the perturbations caused by the planet’s non-sphericity.³ Thus, a satellite is irregular if its orbital semimajor axis is greater than the *Laplace radius* (defined above in Sect. 3.4, see formula (3.91)), i.e., it satisfies the inequality

$$a \gtrsim r_{\text{L}} \approx \left(J_2 R_{\text{p}}^2 a_{\text{p}}^3 \frac{m_{\text{p}}}{m_{\text{Sun}}} \right)^{1/5} \quad (5.3)$$

(Burns 1986; Nesvorný et al. 2003), where J_2 , R_{p} , a_{p} , and m_{p} are the planet’s parameters: its second zonal harmonic coefficient, mean radius, orbital semimajor axis, mass, respectively; m_{Sun} is the Solar mass.

The Hill and Laplace radii for the Solar system planets are given in Table 5.1. An inspection of this Table testifies that the approximate and rigorous definitions of irregulars are similar indeed: for all giant planets, the value of $r_{\text{L}}/r_{\text{H}}$ belongs to

²The term “prograde” designates the planetocentric motion co-directional with the host planet’s heliocentric orbital motion; “retrograde” designates the motion opposite to the prograde one.

³Note that the given definitions of an irregular satellite apply only to the satellite systems of Jovian planets; otherwise the Moon should be also called irregular.

Table 5.1 Masses, figures, and critical radii for the Solar system planets

Planet	Mass m_p (10^{27} g)	Mean radius R_p (km)	Obliquity ($^\circ$)	$J_2 \cdot 10^6$	$J_4 \cdot 10^6$	r_H/R_p	r_L/R_p
Mercury	0.3301	2440	~ 0.1	60	...	90.4	2.66
Venus	4.8673	6052	177.3	4	2	167	2.24
Earth	5.9722	6371	23.45	1083	-2	235	8.41
Mars	0.64169	3390	25.19	1960	-19	320	11.4
Jupiter	1898.1	69,911	3.12	14,696	-587	743	35.4
Saturn	568.32	58,232	26.73	16,291	-915	1080	48.4
Uranus	86.810	25,362	97.86	3343	-29	2680	64.0
Neptune	102.41	24,622	29.56	341	-35	4600	93.2

Notes: Obliquity is the angle between the planet's equatorial and orbital planes; J_2 and J_4 are the second and fourth zonal harmonic coefficients; r_H and r_L are the Hill and Laplace radii. The Table is compiled based on data given in the JPL Database (<http://jpl.nasa.gov/>), Murray and Dermott (1999), and Tremaine et al. (2009). The values of r_H and r_L for Mercury, Venus, Earth, and Mars are given as calculated by the author. The stated value of r_L for the Earth is formal because the Lunar perturbations are not taken into account

the interval between 0.02 and 0.05. It is interesting that, in case the rocky planets also had irregulars, the approximate definition of irregulars for them would be still valid: as follows from the Table, for Mercury, Earth, and Mars, r_L/r_H is still in the range 0.02–0.05, for Venus it is 0.013. Thus, all planets in the Solar system have similar (by the order of magnitude) values of r_L/r_H . The basic reason is that r_L and r_H depend on the planetary parameters rather weakly.

The irregular satellites are mostly small in size, their diameters $D \sim 1\text{--}10$ km. However, each giant planet has one irregular moon with $D > 100$ km, these moons are: JVI Himalia, SIX Phoebe, UXVII Sycorax, and NII Nereid. Nereid is the largest one ($D \approx 340$ km).

The irregulars comprise the majority (in number, but not in mass) of the total satellite population in the Solar system: ~ 110 out of the total count of ~ 170 (as known in the year of publication of this book).

As we shall see in this Chapter, the orbital distributions of irregulars around parent planets are controlled by the LKE. As established by Carruba et al. (2002) and Nesvorný et al. (2003), the most general property of these distributions is that, due to the LKE, most orbits with $i \sim 90^\circ$ are short-lived, and thus no irregular satellites have inclinations in the range between $\sim 50^\circ$ and $\sim 140^\circ$, except two Neptunian moons N9 Halimede and N11 Sao. On the other hand, the secular orbital dynamics of two Saturnian moons S22 Ijiraq and S24 Kiviuq and Jovian moon J34 Euporie is most probably controlled by the LKE.

We consider the irregular satellite systems of Jupiter and Saturn in two separate sections, whereas the satellite systems of Uranus and Neptune are analyzed in a single one, because the two latter systems are mutually similar, though different from the Jovian and Saturnian systems. The major difference is that the non-survivability of orbits due to the LKE occur in the systems of Uranus and Neptune in a narrower inclination range than in the systems of Jupiter and Saturn.

5.1 Irregular Satellites: Origin and Orbits

5.1.1 *Where They Came From*

While the orbits of regular satellites lie deep inside the Hill spheres of their parent planets, the orbits of irregular satellites occupy substantial fractions of inner space of these spheres. What is more, whereas the orbital architecture of regulars is qualitatively similar to that of the Solar system planets (i.e., the orbits are mostly coplanar and close-to-circular), the orbital distributions of the irregulars are strongly disordered.

That is why the origin of irregular satellites is thought to be very different in comparison with that of regulars. The regulars are supposed to be formed in just the same way as planets, i.e., by means of accretion of solids in protodisks (Stevenson et al. 1986). The origin of irregulars seems to be totally different. Indeed, in contrast to regulars, most of them follow retrograde orbits, and this sole fact certifies that they cannot originate from a single nebula. Besides, their eccentricities and inclinations are too large in general to be an outcome of the standard accretion process in a flattened disk.

Therefore, the irregulars are thought to be minor bodies (e.g., asteroids) captured somehow from heliocentric orbits. They had not formed in vicinities of parent planets, but arrived from other realms of the Solar system. Thus, rigorously speaking, the “parent planet” (around which an irregular orbits) is really not a *parent* one. The capture in the three-body problem (the Sun–planet–asteroid problem, in particular) is a complicated, though a thoroughly studied process; see, e.g., Belbruno (2004). Due to the Hamiltonian nature of the three-body problem, such a capture is reversible, and the captured body is doomed to become free again, sooner or later. To make the capture irreversible, non-Hamiltonian perturbations (e.g., gas drag or light pressure) ought to be active.

Several mechanisms of transformation of a body-intruder into an irregular have been proposed: *collisional scenario* (Colombo and Franklin 1971; Gladman et al. 2001), *pull-down capture* (Heppenheimer and Porco 1977; Saha and Tremaine 1993), and *gas-drag capture* (Pollack et al. 1979, 1991). The collisional scenario postulates a disruption of a parent regular satellite by a body passing in a heliocentric orbit; this explains naturally that irregulars cluster in swarms of bodies with similar orbital elements. In the pull-down capture scenario, a body coorbital with a planet is captured by the planet due to mass growth of the latter, as the planet accretes matter at an early stage of its cosmogonical evolution and its Hill sphere swells. In the gas-drag capture scenario, an outer body enters the planet’s gas envelope (also at an early evolutionary stage) and slowly spirals down; when the gas depletes, the orbit “freezes”.

5.1.2 Orbital Distributions

As established already in the beginning of 2000s, there exists a broad gap in the inclination distribution (with respect to the ecliptic plane) of the known irregular satellites: almost no object has the inclination in the range between $\approx 50^\circ$ and $\approx 140^\circ$; see Fig. 5.1. A plausible explanation of this fact is that orbits with $i \sim 90^\circ$ are subject to destruction due to the LKE (Carruba et al. 2002; Nesvorný et al. 2003).

The LKE can produce this gap in two ways (Carruba et al. 2002): (1) the pericenter distance $q = a(1 - e)$ may decrease until the orbit starts to cross the orbits of massive inner regular moons (e.g., the orbit of Callisto in the case of the Jovian system), or even until it falls on the parent planet, i.e., until the equality $q = R_p$ starts to hold, where R_p is the planet’s radius; (2) the apocenter distance $Q = a(1 + e)$

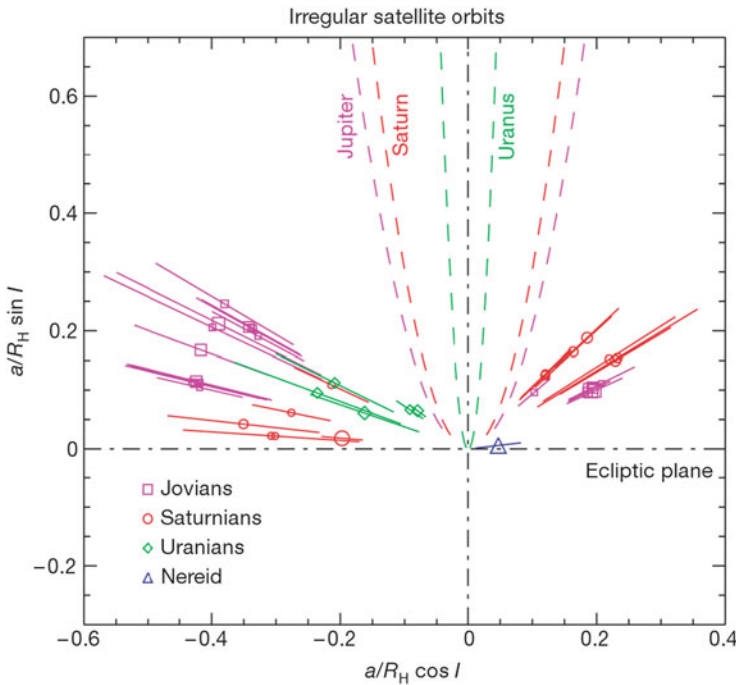


Fig. 5.1 The irregular moons (known up to 2002) of Jupiter, Saturn, Uranus, and Neptune, presented in “polar coordinates”: the angular position (with respect to the horizontal axis) of a satellite in the diagram is equal to the satellite’s inclination i to the ecliptic plane, and the radial position is equal to the satellite’s orbital semimajor axis a in units of the parent planet’s Hill radius R_H . The center-pointing straight line intervals represent the pericenter–apocenter variations in the orbital radii. The symbol size characterizes physical sizes of the moons, namely, diameters in the logarithmic scale. The moons on the right side of the diagram are prograde, and those on the left side are retrograde. A broad gap in the inclinations, centered on $i = 90^\circ$, is evident. The *dashed curves* indicate the borders of the regions where any satellite in a close-to-polar orbit is removed by the LKE (Figure 1 from Gladman et al. (2001). With permission from Nature Publishing Group)

may increase up to $Q \sim R_H$ (the Hill radius), where Solar perturbations destabilize the orbit.

At present, this cosmogonical process is over: Nesvorný et al. (2003) performed long-term numerical integrations of the orbits of all known (at that time) irregulars, taking into account all relevant perturbations, and showed that the known irregular moons are dynamically long-lived.

5.2 Jovian System

Jupiter has 59 irregulars, among them only 7 prograde (see Table 5.2). They form several swarms consisting of moons with similar orbital elements. For example, the Himalia group comprises five moons with semimajor axes $a \sim 0.2R_H$ (where R_H is Jupiter's Hill radius, $R_H = 51 \text{ mln km} = 0.34 \text{ AU}$), eccentricities $e \sim 0.2$, and inclinations $i \sim 30^\circ$ (see Table 5.2). This similarity certifies their common (most probably collisional) origin. The Ananke, Carme, and Pasiphae groups contain moons of smaller physical sizes, but comprise more than a dozen members each.

Note that the inclination values cited in this chapter for irregulars of all planets are all measured with respect to the local *Laplace plane*, defined in Sect. 3.4. Irregulars usually have orbits much greater in size than the *Laplace radius* (also defined in Sect. 3.4; for its specific planetary values see Table 5.1). At such large distances, the Laplace plane coincides approximately with the ecliptic plane.

Carruba et al. (2002) performed massive numerical experiments, integrating orbits of a variety of hypothetical Jovian satellites on a long timescale (10^9 years). It turned out that the LKE due to the Solar perturbations plays the most prominent role in the secular orbital evolution, either driving the pericenters of the satellites with $70^\circ \lesssim i \lesssim 110^\circ$ into the domain of massive regulars (where the satellites are eliminated on the timescale of 10^7 – 10^9 years, due to collisions or gravitational scattering), or driving the apocenters of the satellites out of the planet's Hill sphere. When one takes into account all relevant perturbations, the gap broadens up to $55^\circ \lesssim i \lesssim 130^\circ$ (from $\sim 70^\circ \lesssim i \lesssim 110^\circ$).

Thus, the LKE has produced a major “footprint” in the global orbital architecture of the Jovian irregulars. What is more, the LKE seems to be still operational in the orbital dynamics of some of them. Namely, the secular dynamics of the Jovian moon J34 Euporie seems to be controlled by the LKE, the pericenter argument ω librating around 90° with the full amplitude of 60° , nearly constant over 10^8 years (Nesvorný et al. 2003).

Besides, according to Carruba et al. (2002), there exists a “stable phase space” with orbits surviving on the timescale of 10 Myr for any moon trapped in the LK-resonance (i.e., a moon with the pericenter locked in libration around $\pm 90^\circ$). It contains $\sim 10\%$ of all stable orbits, suggesting that at high inclinations there may exist moons that have not yet been discovered.

Based on analytical (in the framework of the double-averaged Hill problem), numerical (direct numerical integrations), and numerical-analytical approaches,

Table 5.2 Irregular moons of Jupiter

Satellite	a (km)	e	i (°)	D (km)
JXVIII Themisto	7,393,216	0.2115	45.762	8
JXIII Leda	11,187,781	0.1673	27.562	16
JVI Himalia	11,451,971	0.1513	30.486	170
JX Lysithea	11,740,560	0.1322	27.006	36
JVII Elara	11,778,034	0.1948	29.691	86
JLIII Dia	12,570,424	0.2058	27.584	4
JXLVI Carpo	17,144,873	0.2735	56.001	3
S/2003 J12	17,739,539	0.4449	142.680	1
JXXXIV Euporie	19,088,434	0.0960	144.694	2
S/2003 J3	19,621,780	0.2507	146.363	2
S/2003 J18	19,812,577	0.1569	147.401	2
S/2011 J1	20,155,290	0.2963	162.8	1
JLII S/2010 J2	20,307,150	0.307	150.4	1
JXLII Thelxinoe	20,453,753	0.2684	151.292	2
JXXXIII Euanthe	20,464,854	0.2000	143.409	3
JXLV Helike	20,540,266	0.1374	154.586	4
JXXXV Orthosie	20,567,971	0.2433	142.366	2
JXXIV Iocaste	20,722,566	0.2874	147.248	5
S/2003 J16	20,743,779	0.3184	150.769	2
JXXVII Praxidike	20,823,948	0.1840	144.205	7
JXXII Harpalyke	21,063,814	0.2440	147.223	4
JXL Mneme	21,129,786	0.3169	149.732	2
JXXX Hermippe	21,182,086	0.2290	151.242	4
JXXIX Thyone	21,405,570	0.2525	147.276	4
JXII Ananke	21,454,952	0.3445	151.564	28
JL Herse	22,134,306	0.2379	162.490	2
JXXXI Aitne	22,285,161	0.3927	165.562	3
JXXXVII Kale	22,409,207	0.2011	165.378	2
JXX Taygete	22,438,648	0.3678	164.890	5
S/2003 J19	22,709,061	0.1961	164.727	2
JXXI Chaldene	22,713,444	0.2916	167.070	4
S/2003 J15	22,720,999	0.0932	141.812	2
S/2003 J10	22,730,813	0.3438	163.813	2
S/2003 J23	22,739,654	0.3930	148.849	2
JXXV Erinome	22,986,266	0.2552	163.737	3
JXLI Aoede	23,044,175	0.6011	160.482	4
JXLIV Kallichore	23,111,823	0.2041	164.605	2
JXXIII Kalyke	23,180,773	0.2139	165.505	5
JXI Carne	23,197,992	0.2342	165.047	46
JXVII Callirrhoe	23,214,986	0.2582	139.849	9
JXXXII Eurydome	23,230,858	0.3769	149.324	3

(continued)

Table 5.2 (continued)

Satellite	a (km)	e	i ($^\circ$)	D (km)
S/2011 J2	23,329,710	0.3867	151.8	1
JXXXVIII Pasithee	23,307,318	0.3288	165.759	2
JLI S/2010 J1	23,314,335	0.320	163.2	2
JXLIX Kore	23,345,093	0.1951	137.371	2
JXLVIII Cyllene	23,396,269	0.4115	140.148	2
JXLVII Eukelade	23,483,694	0.2828	163.996	4
S/2003 J4	23,570,790	0.3003	147.175	2
JVIII Pasiphae	23,609,042	0.3743	141.803	60
JXXXIX Hegemone	23,702,511	0.4077	152.506	3
JXLIII Arche	23,717,051	0.1492	164.587	3
JXXVI Isonoe	23,800,647	0.1775	165.127	4
S/2003 J9	23,857,808	0.2761	164.980	1
S/2003 J5	23,973,926	0.3070	165.549	4
JIX Sinope	24,057,865	0.2750	153.778	38
JXXXVI Sponde	24,252,627	0.4431	154.372	2
JXXXVIII Autonoe	24,264,445	0.3690	151.058	4
JXIX Megaclite	24,687,239	0.3077	150.398	5
S/2003 J2	30,290,846	0.1882	153.521	2

Notes: The Table is compiled based on data given in the JPL Small-Body Database (<http://ssd.jpl.nasa.gov/>). Real and probable ω -librators are distinguished in bold font

Vashkovyakov and Teslenko (2008a) performed a systematic study of the orbital evolution of all irregulars of Jupiter, known up to 2008, and inferred that the Jovian moon J46 Carpo satisfied the Lidov-Kozai *resonance conditions* $c_1 < 3/5$ and $c_2 < 0$ (Vashkovyakov 1999, 2005), where the classical integrals

$$c_1 = (1 - e^2) \cos^2 i, \quad (5.4)$$

$$c_2 = e^2 \left(\frac{2}{5} - \sin^2 i \sin^2 \omega \right) \quad (5.5)$$

(see Equations (3.23) and (3.24) or (5.4) and (5.5)). In the diagrams “ $i-\omega$ ” and “ $i-e$ ” (Fig. 5.2), J46 Carpo is clearly identifiable as an ω -librator. Satellites J34 Euporie, J49 Kore, and S/2003 J3 are very close to ω -libration. By means of monitoring the long-term behaviour of the pericenter argument, Vashkovyakov and Teslenko (2008a) identified J18 Themisto as another ω -librator.

Using new precise data on initial values of elements, Emelyanov and Vashkovyakov (2012) performed direct numerical integrations of non-averaged equations of motion on timescales of several thousand years and showed that J34 Euporie and J46 Carpo were indeed in ω -libration, whereas J18 Themisto and J49 Kore circulated.

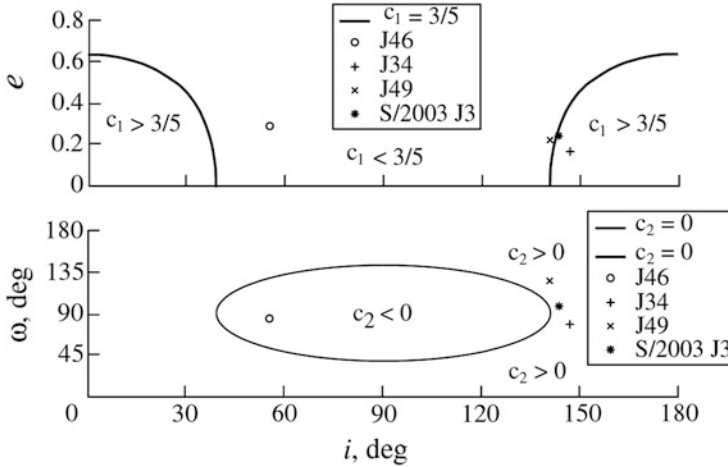


Fig. 5.2 The irregulars of Jupiter in the planes of initial conditions (i_0, e_0) and (i_0, ω_0) . The symbols designate moons, and the curves trace constant values of c_1 (in the *upper panel*) and c_2 (in the *lower panel*). Omega-librators are identified (Figure 55 from Vashkovyak and Teslenko (2008a)). With permission from Pleiades Publishing Inc)

Thus, at least four Jovian moons reside in LK-resonance or are close to it at present. In Table 5.2, those Jovian satellites that are observed to be in ω -libration, or close to this state, are distinguished in bold font.

5.3 Saturnian System

Saturn has 38 irregulars, among which only 9 are prograde (see Table 5.3). In total, Saturn’s irregulars have semimajor axes in the range $0.16\text{--}0.36R_H$, where Saturn’s Hill radius $R_H = 69 \text{ mln km} = 0.46 \text{ AU}$. The Saturnian irregulars form three swarms of moons with similar orbital elements, namely, the Inuit, Norse, and Gallic groups. Some of them were shown to be remnants (most likely) of larger objects, captured by the planet and then collisionally disrupted (Gladman et al. 2001).

In the framework of the double-averaged Hill problem, Vashkovyak (2001) identified ω -libration in the long-term behaviour of S20 Paaliaq, S22 Ijiraq, S24 Kiviuq, and S29 Siarnaq. However, the phase trajectories of S20 Paaliaq and S29 Siarnaq in the “ ω – e ” plane were too close to the LK-separatrix (i.e., $c_2 \approx 0$ for them), and in a more precise model of evolution they turned out to circulate (Vashkovyak 2003).

Nesvorný et al. (2003) performed direct numerical integrations of orbits of the Saturnian moons, monitoring the behaviour of various resonance angles allowed by the D’Alembert rules (defined, e.g., in Morbidelli 2002; see also Ferraz-Mello 2007; Kholshvnikov 1997, 2001). The Lidov-Kozai resonance angle (the pericenter

Table 5.3 Irregular moons of Saturn

Satellite	a (km)	e	i ($^{\circ}$)	D (km)
SXXIV Kiviuq	11,294,800	0.3288	49.087	16
SXXII Ijiraq	11,355,316	0.3161	50.212	12
SIX Phoebe	12,869,700	0.156242	173.047	213
SXX Paaliaq	15,103,400	0.3631	46.151	22
SXXXVII Skathi	15,672,500	0.246	149.084	8
SXXXVI Albiorix	16,266,700	0.477	38.042	32
S/2007 S2	16,560,000	0.2418	176.68	6
SXXXVII Bebhionn	17,153,520	0.333	40.484	6
SXXXVIII Erriapus	17,236,900	0.4724	38.109	10
SXLVII Skoll	17,473,800	0.418	155.624	6
SXXXIX Siarnaq	17,776,600	0.24961	45.798	40
SLII Tarqeq	17,910,600	0.1081	49.904	7
S/2004 S13	18,056,300	0.261	167.379	6
SLI Greip	18,065,700	0.3735	172.666	6
SXLIV Hyrrokkin	18,168,300	0.3604	153.272	8
SL Jarnsaxa	18,556,900	0.1918	162.861	6
SXXI Tarvos	18,562,800	0.5305	34.679	15
SXXV Mundilfari	18,725,800	0.198	169.378	7
S/2006 S1	18,930,200	0.1303	154.232	6
S/2004 S17	19,099,200	0.226	166.881	4
SXXXVIII Bergelmir	19,104,000	0.152	157.384	6
SXXXI Narvi	19,395,200	0.320	137.292	7
SXXIII Suttungr	19,579,000	0.131	174.321	7
SXLIII Hati	19,709,300	0.291	163.131	6
S/2004 S12	19,905,900	0.396	164.042	5
SXL Farbauti	19,984,800	0.209	158.361	5
SXXX Thrymr	20,278,100	0.453	174.524	7
SXXXVI Aegir	20,482,900	0.237	167.425	6
S/2007 S3	20,518,500	0.130	177.22	5
SXXXIX Bestla	20,570,000	0.5145	147.395	7
S/2004 S7	20,576,700	0.5299	165.596	6
S/2006 S3	21,076,300	0.4710	150.817	6
SXLI Fenrir	21,930,644	0.131	162.832	4
SXLVIII Surtur	22,288,916	0.3680	166.918	6
SXLV Kari	22,321,200	0.3405	148.384	7
SXIX Ymir	22,429,673	0.3349	172.143	18
SXLVI Loge	22,984,322	0.1390	166.539	6
SXLII Fornjot	24,504,879	0.186	167.886	6

Note: The Table is compiled based on data given in the JPL Small-Body Database (<http://ssd.jpl.nasa.gov/>). Real and probable ω -librators are distinguished in bold font

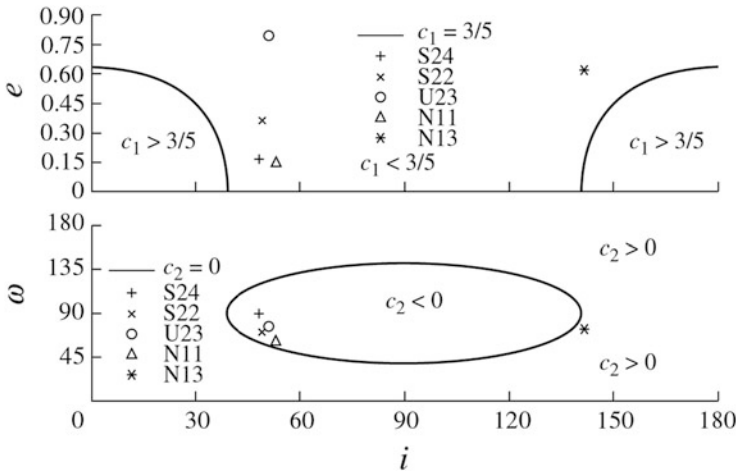


Fig. 5.3 The irregulars of Saturn, Uranus, and Neptune in the planes of initial conditions (i_0, e_0) and (i_0, ω_0). The symbols designate moons, and the curves trace constant values of c_1 (in the upper panel) and c_2 (in the lower panel). Omega-librators are identified (Figure 53 from Vashkovyak and Teslenko (2008b)). With permission from Pleiades Publishing Inc

argument) was monitored in particular. It was found that the LKE controls the secular orbital dynamics of two Saturnian moons, namely, S22 Ijiraq and S24 Kiviuq: the pericenter argument ω librates in both cases around 90° with the full amplitude of 60° , nearly constant over 10^8 years, certifying that this resonant behaviour is very likely primordial.

Vashkovyak and Teslenko (2008b) integrated numerically the orbits of all irregulars of Saturn, known up to 2008, and confirmed that the moons S22 Ijiraq and S24 Kiviuq satisfied the Lidov-Kozai resonance conditions $c_1 < 3/5$ and $c_2 < 0$ (Equations (3.23) and (3.24) or (5.4) and (5.5)). In the diagrams “ $i-\omega$ ” and “ $i-e$ ” (Fig. 5.3), the ω -librators are identified. One can see that S20 Paaliaq is close to ω -libration. In Table 5.3, those Saturnian satellites that are observed to be in ω -libration, or close to this state, are distinguished in bold font.

5.4 Uranian and Neptunian Systems

The Uranian and Neptunian systems are mutually similar, but they are not like those described above. The major difference in comparison with the Jovian and Saturnian systems is that the instabilities due to the LKE occur in a narrower inclination range.

Uranus has nine irregulars, all retrograde except one (U23 Margaret, see Table 5.4). Their semimajor axes are in the range $0.06-0.29R_H$, where Uranus’s Hill radius $R_H = 73 \text{ mln km} = 0.49 \text{ AU}$. In contrast to the Jovian and Saturnian systems, a large and uniform spread of the moons in the semimajor axis does not

Table 5.4 Irregular moons of Uranus

Satellite	a (km)	e	i ($^\circ$)	D (km)
UXXII Francisco	4,276,000	0.1459	147.459	22
UXVI Caliban	7,230,000	0.1587	139.885	72
UXX Stephano	8,002,000	0.2292	141.873	32
UXXI Trinculo	8,571,000	0.2200	166.252	18
UXVII Sycorax	12,179,000	0.5224	152.456	150
UXXIII Margaret	14,345,000	0.6608	51.455	20
UXVIII Prospero	16,418,000	0.4448	146.017	50
UXIX Setebos	17,459,000	0.5914	145.883	48
UXXIV Ferdinand	20,900,000	0.3682	167.346	20

Note: The Table is compiled based on data given in the JPL Small-Body Database (<http://ssd.jpl.nasa.gov/>). Real and probable ω -librators are distinguished in bold font

Table 5.5 Irregular moons of Neptune

Satellite	a (km)	e	i ($^\circ$)	D (km)
NII Nereid	5,513,818	0.7507	7.090	340
NIX Halimede	16,611,000	0.2646	112.898	62
NXI Sao	22,228,000	0.1365	49.907	44
NXII Laomedeia	23,567,000	0.3969	34.049	42
NX Psamathe	48,096,000	0.3809	137.679	40
NXIII Neso	49,285,000	0.5714	131.265	60

Note: The Table is compiled based on data given in the JPL Small-Body Database (<http://ssd.jpl.nasa.gov/>). Real and probable ω -librators are distinguished in bold font

allow one to identify any clustering that would suggest a common origin for a group of objects; i.e., the Uranian moons, most probably, have formed independently from each other.

Neptune has 6 irregulars, among which 3 are prograde and 3 retrograde (see Table 5.5), with semimajor axes $0.05\text{--}0.42R_H$, where Neptune's Hill radius $R_H = 116$ mln km = 0.78 AU. Neptune's most famous (due to its record eccentricity $e \approx 0.75$) irregular moon N2 Nereid is prograde. Goldreich et al. (1989) suggested that Nereid's high eccentricity is due to perturbations of formerly captured Triton. While migrating, Triton might have also disrupted orbits of other satellites of Neptune, if they have ever existed.

The orbital distributions of the Uranian and Neptunian moons (except two Neptunian moons N9 Halimede and N11 Sao) are consistent with the broad gap in the compiled inclination distribution⁴ of the known irregulars in the Jovian and Saturnian systems: no object has inclination in the range between $\approx 50^\circ$ and $\approx 140^\circ$. Again, a plausible explanation is that most orbits with $i \sim 90^\circ$ are unstable due to the LKE (Carruba et al. 2002; Nesvorný et al. 2003).

⁴With respect to the ecliptic plane.

Vashkovyakh and Teslenko (2008b) integrated numerically the orbits of all irregulars of Uranus and Neptune, known up to 2008, and inferred that U23 Margaret and N11 Sao satisfied the Lidov-Kozai resonance conditions $c_1 < 3/5$ and $c_2 < 0$. In the diagrams “ $i-\omega$ ” and “ $i-e$ ” (Fig. 5.3), the ω -librators are identified. N13 Neso is apparently close to ω -libration. In Tables 5.4 and 5.5, those Uranian and Neptunian satellites that are observed to be in ω -libration, or close to this state, are distinguished in bold font.

Finally, note that if an additional perturbation dominates over the LK-term in the Hamiltonian of the motion, then the LKE may be quenched, as discussed above in Sect. 3.3. Such a suppression explains, e.g., the stable existence of *regular* satellites of Uranus (Lidov 1963b). The regular Uranian moons move in orbits close to the planet’s equatorial plane, which is inclined by 98° with respect to the orbital plane. The LKE driven by Solar perturbations would enforce the satellites to fall onto the planet, but this does not occur because the frequencies of orbital precession (caused by the planet’s oblateness and mutual perturbations between the moons) are large enough to suppress the LKE.